arXiv:nucl-th/0106039v1 18 Jun 2001

Meson Properties in Dense Hadronic Matter

J. Wambach[a]*,

[a] Institut für Kernphysik, Technische Universität Darmstadt,
Schloßgartenstr. 9, D-64289 Darmstadt, Germany

The medium modification of mesons in dense hadronic matter is discussed with a focus on the relationship to the chiral structure of the non-perturbative QCD vacuum.

1. INTRODUCTION

One of the fundamental questions in strong interaction physics concerns the generation of mass in the sector of light quarks. How can nucleons with a mass of roughly 1 GeV arise from up and down quark masses of less than 10 MeV? The answer lies in the non-perturbative structure of the QCD vacuum itself in which quarks and gluons condense. This is in marked contrast to the heavy-quark sector where the masses of the hadrons are determined by the quark masses themselves. These, in turn, are set at the electroweak scale through the Higgs mechanism.

When nuclear matter is subjected to extreme conditions in density and temperature such as in the interior of neutron stars or in central relativistic heavy-ion collisions, the QCD vacuum will be altered, eventually leading to the liberation of the elementary constituents in a new state of matter, the 'quark gluon plasma' (QGP). Such a restructuring of the vacuum must be accompanied by significant changes in the spectral properties of hadrons, commonly called 'medium modifications'. Here mesons are of particular importance, since they constitute the 'elementary' $\bar{q}q$ excitations of the vacuum and hence serve as experimental probes of the underlying vacuum changes. For the structure of light mesons chiral symmetry and its spontaneous break-down plays a decisive role as is well established from lattice QCD simulations [1]. The physical mechanism for spontaneous symmetry breaking and mass generation is provided by instantons which largely saturate the euclidian gauge-field action [2]. These induce effective quark-(anti)quark interactions which are strong enough to cause a BCS-like transition [3] to a $\bar{q}q$ condensate. As a result a mass gap appears, the 'constituent quark' mass of $\sim$ 300-500 MeV. It has been demonstrated that this picture yields an excellent description of hadronic correlation functions [2] and hence forms the basis for a variety of approaches to deal with medium modifications. An obvious starting point is NJL-type models [3] where the instanton-induced interaction is assumed to be point-like. They are very successful in describing mesonic spectral functions, especially when treated beyond the mean-field approximation [4]. Such calculations are very demanding but finally lead to results in accordance with 'effective theories' (such

*This work was supported by GSI and BMBF

as the vector dominance model (VDM) [5]) in which hadronic fields feature as the elementary degrees of freedom. It is more 'economical' to start with those from the outset, especially when dealing with 'precursor' phenomena of the QGP transition. This strategy will be followed in the present contribution.

2. CHIRAL EFFECTIVE THEORY AND CORRELATORS

The spontaneous breaking of chiral symmetry has two important consequences. One is the appearance of massless Goldstone bosons and the other is the absence of parity doublets in the hadron spectrum ($m_\pi \neq m_{f_0}, m_\rho \neq m_{a_1}$ etc). For the present discussion the second will be more relevant. Chiral symmetry does, however, more than just predict the existence of Goldstone bosons. It also prescribes and severely restricts their mutual interactions as well as those with other hadrons. This forms the basis for constructing 'chiral effective theories'.

The formal starting point are the pertinent quark currents

$$J_i(x) = \bar{q}(x)\Gamma_i q(x), \Gamma_i = 1, \gamma_5, \gamma_\mu, .. \tag{1}$$

which are identified with *elementary* hadronic fields $\phi_i(x)$. One then writes down the most general effective Lagrangian, consistent with the underlying symmetries and anomaly structure of QCD. Relevant examples are the linear- or nonlinear sigma model, gauged sigma models, etc.

The physical information about hadronic spectral properties and their in-medium modification is contained in the current-current correlation functions $D_i(x) \propto \langle J_i(x)J_i(0)\rangle$. In terms of the elementary hadronic fields and for matter in thermal and chemical equilibrium they are given by the (retarded) momentum-space Green's function

$$D_i(\omega, \vec{q}) = i\int d^4x \, e^{iqx}\theta(x_0)\langle\langle[\phi_i(x), \phi_i(0)]\rangle\rangle \tag{2}$$

where the average is taken in the grand canonical ensemble. All information about the physical excitations of the medium is contained in the spectral function

$$A_i(\omega, \vec{q}) = -\frac{1}{\pi}\mathrm{Im}D_i(\omega, \vec{q})\,. \tag{3}$$

In the first step the parameters of the chiral Lagrangian are adjusted to reproduce the vacuum properties of the hadronic correlators in question (mass, width..) as well as possible. Here either perturbative, or in some cases, non-perturbative methods [6] are used. Once the vacuum model is fixed, the medium modifications can be predicted with a good degree of accuracy.

3. MESONS IN THE HADRONIC MEDIUM

3.1. Chiral Condensate evolution

With increasing density (baryo-chemical potential μ_q) and temperature T the quark condensate will diminish and eventually vanish, thus restoring chiral symmetry. For hadronic matter in equilibrium the QCD partition function is given by

$$\mathcal{Z}_{QCD}(V, T, \mu_q) = \mathrm{Tr} e^{-(H_{QCD}-\mu_q N_q)/T}, \tag{4}$$

where N_q is the quark number operator and μ_q the quark chemical potential. The quark condensate $\langle\langle\bar{q}q\rangle\rangle$ can be directly inferred from the free energy density in the thermodynamic limit

$$\Omega_{QCD}(T,\mu_q) = -\lim_{V\to\infty}\frac{T}{V}\ln \mathcal{Z}_{QCD}(V,T,\mu_q) \quad \text{as} \quad \langle\langle\bar{q}q\rangle\rangle = \frac{\partial\Omega_{QCD}(T,\mu_q)}{\partial m_q^\circ} \ , \tag{5}$$

where m_q° denotes the current quark mass.

In the broken phase, the obvious first step is to approximate the free energy density by an ideal gas of hadrons. The resulting in-medium condensate then becomes

$$\frac{\langle\langle\bar{q}q\rangle\rangle}{\langle\bar{q}q\rangle} = 1 - \sum_h \frac{\Sigma_h \varrho_h^s(T,\mu_q)}{f_\pi^2 m_\pi^2}; \quad \Sigma_h = m_q^\circ \frac{\partial m_h}{\partial m_h^\circ} \tag{6}$$

where ϱ_h^s denotes the scalar density of hadrons and m_h their vacuum mass. At low temperature and small μ_q in which the hadron gas is dominated by thermally excited pions and a free Fermi gas of nucleons, Eq. (6) leads to the model-independent leading-order result

$$\frac{\langle\langle\bar{q}q\rangle\rangle}{\langle\bar{q}q\rangle} = 1 - \frac{T^2}{8f_\pi^2} - 0.3\frac{\rho}{\rho_0}\dots \ , \tag{7}$$

where $\rho_0 = 0.16/\text{fm}^3$ is the saturation density of symmetric nuclear matter. Thus the mere presence of an ideal gas of hadrons already alters the vacuum and leads to a decrease of the condensate, without changing the vacuum properties of the hadrons! Obviously medium-modifications and the corresponding non-trivial change of the QCD vacuum have to involve hadronic interactions. They become increasingly important as the matter grows hotter and denser, i.e. as the point of chiral restoration is approached. The theoretical description involves more and more degrees of freedom, which severely limits the description in terms of elementary hadronic fields near the phase transition.

3.2. Fluctuations of the chiral condensate

Being dependent on the renormalization scale, the chiral condensate is not observable. However, the fluctuations $\langle\langle(\bar{q}q)^2\rangle\rangle - \langle\langle\bar{q}q\rangle\rangle^2$ are. They correspond to the scalar (chiral) susceptibility and are given as the second derivative of the free energy density

$$\chi_+ = \langle\langle(\bar{q}q)^2\rangle\rangle - \langle\langle\bar{q}q\rangle\rangle^2 = \frac{\partial^2\Omega_{QCD}(T,\mu_q)}{\partial^2 m_q^\circ} \tag{8}$$

w.r.t. to the current quark mass. To make contact with the hadronic spectrum we consider the bilinear scalar quark current $J_+ = \bar{q}q$. From the corresponding correlator

$$D_+(\omega,\vec{q}) = i\int d^4x\,\theta(x_0)e^{iqx}\langle\langle[(J_+(x),J_+(0)]\rangle\rangle \ . \tag{9}$$

the scalar susceptibility is obtained as the 'polarizability sum rule' for the scalar spectral function $A_+(\omega,\vec{q})$:

$$\chi_+ = \int_0^\infty d\omega A_+(\omega,\vec{q}=0) \ , \tag{10}$$

and hence relates to the properties of the scalar f_0 meson in the medium.

From direct lattice simulations it is established that QCD with two flavors and vanishing μ_q exhibits a second-order phase transition in the chiral limit [7]. The transition at $T = 0$ but finite μ_q is not as well understood, since it cannot be simulated on the lattice, due to complex fermion determinants. Model calculations indicate however that it may be first order at several times ρ_0. As a second- or weak first-order phase transition is approached the fluctuations of the order parameter become large. A measure for the growth are the appropriate susceptibilities which, in a second-order transition, diverge with critical exponents that are determined by universal behavior. The approach to criticality in the case of two-flavor QCD is clearly seen on the lattice [8].

Following the suggestion in ref. [9] that two-flavor QCD lies in the same universality class as the $O(4)$ Heisenberg model we can use the linear sigma model to asses the chiral fluctuations in the hadronic medium. In this case the scalar correlator D_+ in Eq. (9) is identified with the in-medium σ-propagator:

$$D_+ = D_\sigma(\omega, \vec{q}) = i \int d^4x e^{iqx} \theta(x_0) \langle\langle [\sigma(x), \sigma(0)] \rangle\rangle \, . \tag{11}$$

Applying a low-density expansion for the in-medium condensate according to Eq. (7)

$$\langle\langle \sigma \rangle\rangle \equiv \langle \sigma \rangle \Phi(\rho); \quad \Phi(\rho) = 1 - \alpha \frac{\rho}{\rho_0} \tag{12}$$

together with pionic loop corrections the results [10] depicted in Fig. 1 predict a dramatic

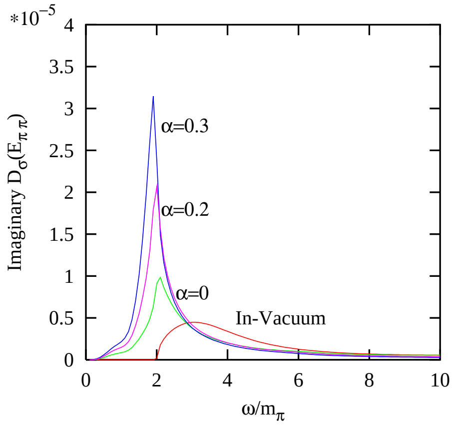

Figure 1. The imaginary part of $D_\sigma(\omega, 0)$ [10] at nuclear saturation density for various values of α, the parameter that controls the linear density dependence of $\langle\langle \sigma \rangle\rangle$ (Eq. 7).

near-threshold enhancement of the σ spectral function already at ρ_0 (corresponding to $\Phi(\rho) \sim 0.7 - 0.8$). It should be noted that this effect is also found in the non-linear realization of chiral symmetry [11] and is therefore generic.

What are the experimental signatures? Since the σ meson strongly couples to two-pion states an obvious experiment is the production of two $J = I = 0$ pions near threshold in

nuclei. Such experiments have been conducted by the CHAOS collaboration at TRIUMF using an incident π^+ beam on various nuclear targets [12] identifying charged pions in the final state. A second experiment is by the Crystal Ball (CB) collaboration at BNL with an incident π^- beam [13] detecting a π^0 pair in the final state through coincident 4γ decay. For the invariant mass distribution of the produced pion pair both measurements consistently observe a significant reshaping as function of mass number as indicated in Fig 2. Here the composite ratio

$$C^A_{\pi\pi} = \frac{\sigma^A(M_{\pi\pi})}{\sigma^A_T} / \frac{\sigma^N(M_{\pi\pi})}{\sigma^N_T} \ , \tag{13}$$

is displayed, where $\sigma^A(M_{\pi\pi})$ ($\sigma^N(M_{\pi\pi})$) denotes the invariant mass distribution in the nucleus (nucleon), while σ^A_T (σ^N_T) is the corresponding total cross section for the $\pi 2\pi$ process. The various curves in the left panel of Fig. 3 reflect the theoretical predictions.

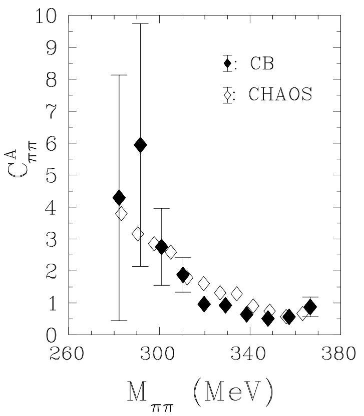

Figure 2. The composite ratio $\mathcal{C}^A_{\pi\pi}$ for ^{12}C [14].

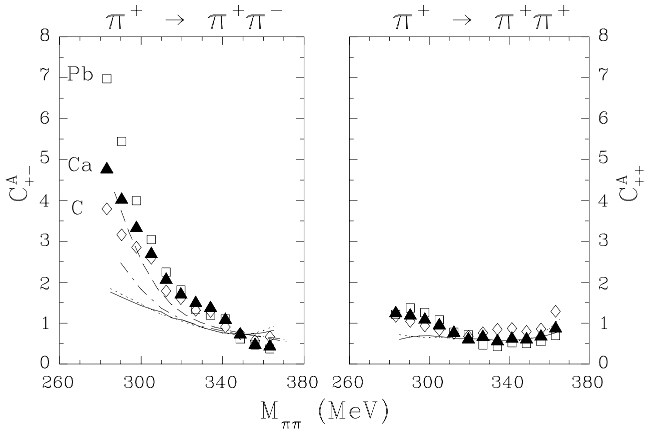

Figure 3. The composite ratio $C^A_{\pi\pi}$ for various nuclear targets [15].

The full [16] and dotted [17] lines only include contributions from p-wave modifications of the pion propagator while the dashed-dotted line [18] only considers the dropping of the σ mass without dressing the pion loop. Finally the dashed line [10] includes both effects and gives a reasonable description of the data.

3.3. The ρ meson and Dileptons

The ρ meson is featured as a prominent resonance in the e^+e^- annihilation cross section and therefore plays a central role for dilepton production in heavy-ion collisions at invariant masses below 1GeV. In general, the production rate is given in terms of the in-medium electromagnetic current-current correlation function as

$$\frac{dR_{l^+l^-}}{d^4q} = f(q_0) L^{\mu\nu} \mathrm{Im} D^{\mathrm{elm}}_{\mu\nu}; \quad D^{\mathrm{elm}}_{\mu\nu}(\omega, \vec{q}) = -i \int d^4x \, e^{iqx} \theta(x_0) \langle\langle [J^{\mathrm{elm}}_\mu(x), J^{\mathrm{elm}}_\nu(0)] \rangle\rangle \tag{14}$$

where $L^{\mu\nu}$ denotes the lepton tensor and $f(q_0)$ is a thermal Bose factor. Invoking vector dominance, the hadron tensor $D^{\rm elm}_{\mu\nu}$ directly relates to the in-medium properties of the ρ meson and can be evaluated in the VDM. Two important medium effects can be identified. The first is the modification of the intermediate two-pion state to which the ρ meson strongly couples. Here proper care has to be taken to ensure gauge invariance. The second is a direct coupling to baryonic resonances, most prominently the $N^*(1550)$ resonance. The inclusion of both effect leads to a large broadening of the spectral function at high density and temperature and results in a dramatic reshaping of the dilepton rate as indicated in the left panel of Fig. 4. Once the local rate is space-time evolved

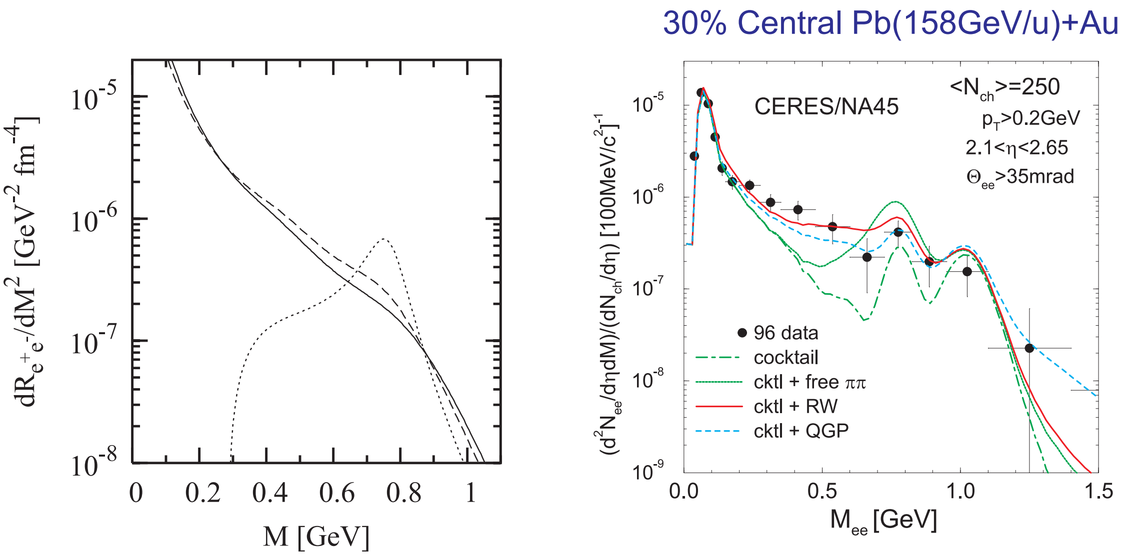

Figure 4. Dilepton rates: the left panel displays the theoretical prediction at T=150 MeV and $\mu_B = 3\mu_q$=452 MeV [19] while the right panel shows a comparison [20] with the measured rates of the CERES collaboration [21].

through a realistic fire ball expansion until thermal freeze out, and detector acceptances and background rates from Dalitz decays are properly accounted for, the resulting rates compare favorably with the measurements of the CERES collaboration at the CERN SpS [21] (right panel of Fig. 4). Also the transverse spectra are well reproduced.

The connection to the restoration of chiral symmetry is not apparent, however. This requires a simultaneous evaluation of both the vector- and axialvector correlator. In the vacuum and in the chiral limit both are related by two 'Weinberg sum rules' [22]:

$$\int_0^\infty ds\,(\rho^\circ_V(s) - \rho^\circ_A(s)) = f_\pi^2; \qquad \int_0^\infty dss\,(\rho^\circ_V(s) - \rho^\circ_A(s)) = 0 \tag{15}$$

where the first directly links the vacuum spectral functions to f_π, the order parameter of chiral symmetry restoration. Similar sum rules also hold in the hadronic medium [23]

and serve as an important constraint of models that intend to properly implement chiral symmetry in the correlators. One such model has recently been proposed in ref. [24]. The starting point is the linear sigma model (a non-linear realization of chiral symmetry could also be chosen). Combining the ρ- and a_1 fields as chiral partners

$$Y^\mu = \vec{\rho}^\mu \cdot \vec{T} + \vec{a}_1^\mu \cdot \vec{T}_5 \tag{16}$$

one then writes down the most general Lagrangian consistent with *global* chiral symmetry to a given order in the derivative coupling. This introduces a set of bare parameters to be determined from the vacuum phenomenology, in particular the measured vector- and axialvector spectral functions. In the one-loop approximation one can achieve an excellent description of the pion electromagnetic form factor, p-wave $\pi\pi$ phase shifts, e^+e^- cross sections and τ-decay [24]. The extension to finite temperature is straightforward and results in the spectral distributions displayed in Fig. 5 for the chiral limit. At high

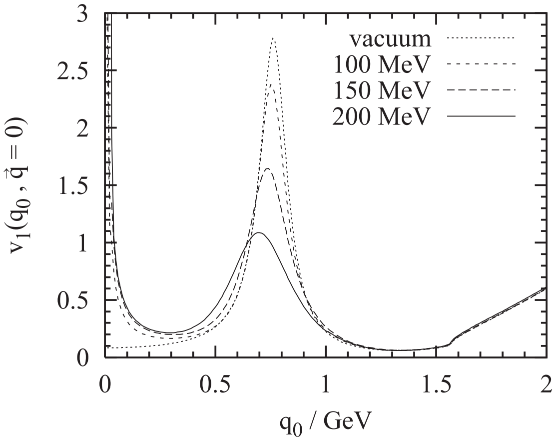

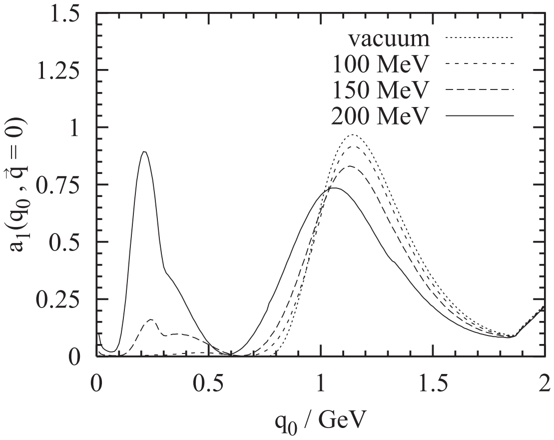

Figure 5. The temperature dependence of the vector spectral function (left panel) and the axialvector spectral function (right panel) in the chiral limit [25].

temperatures a significant reshaping of the strength distribution is observed, especially at low energy. Nonetheless the ρ and a_1 peak remain present, even in the vicinity of the phase boundary. The parameters of the model Lagrangian can be easily adjusted so that, at tree level, the ρ-meson mass is proportional to the chiral condensate $\langle\langle\sigma\rangle\rangle$. This is the scenario of 'Brown-Rho scaling' [26]. To one-loop order, however, it can be proven analytically that the pole mass of the ρ meson remains unchanged to order T^2 and only receives contributions of order T^4 and higher hence invalidating the 'Brown-Rho scenario'.

4. SUMMARY

Based on general considerations of spontaneous breaking of chiral symmetry and its restoration in hot and dense hadronic matter we have discussed the in-medium properties

of σ- and ρ mesons. The former relate to the increased fluctuations of the chiral order parameter which are accessible through measurements of s-wave isoscalar two-pion correlations in nuclei. Interesting near-threshold enhancements in the invariant-mass distribution are observed in $\pi 2\pi$ reactions, which can be interpreted as a signal of the partial restoration of chiral symmetry. The ρ meson and its medium modification plays an important role in the dilepton production in relativistic heavy-ion collisions. Realistic calculations of the spectral function in a hot and dense fireball indicate a significant broadening due to collisions with baryons and mesons and explain the observed production rates. The relation to chiral symmetry is not obvious, however. To address this issue one has to consider the vector- and axialvector correlators simultaneously. Invoking global chiral symmetry in constructing a chiral Lagrangian from elementary σ, π, ρ and a_1 fields it can be shown that, in the chiral limit, there is no direct relationship between the pole mass of the ρ meson and the chiral condensate.

REFERENCES

1. J. W. Negele, Nucl. Phys. Proc. Suppl. 73 (1999) 92.
2. T. Schäfer, E. V. Shuryak, Rev. Mod. Phys. 70 (1998) 323.
3. Y. Nambu and G. Jona-Lasinio, Phys. Rev. 122 (1961) 345.
4. M. Oertel, M. Buballa, J. Wambach, Nucl. Phys. A676 (2000) 247;
   M. Oertel, M. Buballa, J. Wambach, hep-ph/0008131.
5. J. J. Sakurai, Ann. Phys. 11 (1960) 1.
6. Z. Aouissat, P. Schuck, J. Wambach, Nucl. Phys. A618 (1997) 402.
7. F. Karsch, hep-ph/0103314.
8. F. Karsch, Nucl. Phys. A590 (1995) 367.
9. R. Pisarski, F. Wilczek, Phys. Rev. D29 (1984) 338.
10. Z. Aouissat, G. Chanfray, P. Schuck, J. Wambach, Phys. Rev. C61 (2000) 12202.
11. D. Jido, T. Hatsuda, T. Kunihiro, hep-ph/0008076.
12. F. Bonutti et al., Phys. Rev. Lett. 77 (1996) 603.
13. A. B. Starostin et al., Phys. Rev. Lett. 85 (2000) 5539.
14. P. Camerini et al., submitted to Phys. Rev. C.
15. F. Bonutti et al., Nucl. Phys. A677 (2000) 213.
16. M. J. Vicente Vacas, E. Oset, Phys. Rev. C60 (1999) 64621.
17. R. Rapp et al., Phys. Rev. C59 (1999) R1237.
18. T. Hatsuda, T. Kunihiro, H. Shimizu, Phys. Rev. Lett. 82 (1999) 2840.
19. M. Urban, M. Buballa, J. Wambach, Nucl. Phys. A673 (2000) 357.
20. R. Rapp, J. Wambach, Adv. Nucl. Phys. 25 (2000) 1.
21. G. Agakichiev et al., Phys. Rev. Lett. 75 (1995) 1272.
22. S. Weinberg, Phys. Rev. Lett. 18 (1967) 507.
23. J. Kapusta, E. V. Shuryak, Phys. Rev. D49 (1994) 4694.
24. M. Urban, M. Buballa, J. Wambach, hep-ph/0102260.
25. M. Urban, M. Buballa, J. Wambach, work in progress.
26. G. E. Brown, M. Rho, Phys. Rev. Lett. 66 (1991) 2720.